

## FURTHER DEVELOPMENT OF SNL-SWAN, A VALIDATED WAVE ENERGY CONVERTER ARRAY MODELING TOOL

Aaron Porter  
Coast and Harbor Engineering  
Edmonds, WA, U.S.A

Kelley Ruehl  
Sandia National Laboratories  
Albuquerque, New Mexico, U.S.A

Chris Chartrand  
Sandia National Laboratories  
Albuquerque, New Mexico, U.S.A

### ABSTRACT

Commercialization of wave energy will lead to the necessary deployment of Wave Energy Converters (WECs) in arrays, or wave farms. In order for projects in the United States to be approved, regulatory agencies must perform an Environmental Assessment proving little to no environmental impact. However, little is known about the environmental impacts of such wave farms. As a result, the environmental impacts of wave farms are largely determined by numerical wave models capable of modeling large areas (i.e., spectral wave models). However spectral wave models are currently limited in their ability to model WECs. Sandia National Laboratories is developing SNL-SWAN, a modified version of Simulation WAVes Nearshore [1] that includes a validated WEC Module to more realistically model the frequency and sea state dependent wave energy conversion of WECs. This paper will provide an update on its development.

### INTRODUCTION

Accurately assessing potential far-field environmental impacts due to wave energy converter (WEC) arrays is needed for commercialization of wave energy. Wave energy converters are in various stages of development, with most developers in early Technology Readiness Levels (TRLs), with some developers testing devices in the open ocean. However, utility-scale WEC arrays have not yet made it to the market. One of the barriers to development is how to address environmental concerns related to the impact these arrays will have on the wave climate. For example, in the United States an environmental assessment is needed for all WEC array projects prior to installation, which includes an analysis on wave climate impact. Therefore a validated, publicly available wave model that accurately predicts the effects due to WEC-arrays is crucial to WEC commercialization.

The present, or baseline versions, of wave modeling programs do not have the inherent

capabilities needed for modeling far-field impacts due the deployment of WECs in wave farms. For example, the computational resources required to run a far-field Computational Fluid Dynamics (CFD) model are unrealistic for the industry [2]. Potential flow models such as WAMIT [3] require flat bottom bathymetry and therefore do not accurately model wave propagation to the nearshore [4]. Mild-slope and Boussinesq models are also moderately suitable for modeling the environmental impact of WEC-Arrays [4]; however, typically these models are not open source and have other computational limitations (such as the shallow-water and mild-slope assumptions). Another limiting factor is that baseline versions of spectral wave models such as TOMAWAC [5] and SWAN [6] use a frequency independent treatment of obstacles in the wave field. SWAN is a widely accepted open-source spectral wave modeling tool, and previous WEC modeling work has utilized it. Whereas TOMAWAC is commercially available and not open-source. Therefore source code development of SWAN must be made to customize any far-field modeling effort of WEC arrays. The goal of this work is to have a widely distributed open-source version of SWAN, SNL-SWAN, that can accurately simulate the effects of wave farms on the wave climate through the development of a WEC Module. This paper will outline changes made to the SWAN source code, provide comparisons of SWAN results to existing models, and to an observational data set collected at Oregon State University in 2010-2011 using arrays of Columbia Power Technologies' (ColPwr) now superseded Manta 3.1 device [7].

### BACKGROUND

Presently, the baseline versions of spectral models such as SWAN and TOMAWAC parameterize obstacles by applying a constant transmission coefficient across the entire frequency spectrum. Baseline SWAN has the option of using either the built in obstacle

transmission coefficient ( $K_t$ ), using options such as the Goda (1967), or d'Angremond and Van der Meer formulae (1996). In both of these options the transmission coefficient is intended for a partially blocking breakwater, and applies a calculated  $K_t$  across all frequencies. This method of constant transmission across the frequency spectrum had been applied in initial studies as a first step in evaluating the effects wave farms may have on the coast. For example Millar [6] provided sensitivity analysis of WEC transmissivity at the WaveHub site in Southern England. Venugopal and Smith [8] evaluated wave shadows with porous structures that remove power equally across frequencies using the MIKE21 suite. However studies have shown that a fundamental part of WECs is that they do not remove wave power equally across all frequencies [9-10]

Several studies implementing frequency dependent WEC parameterizations to examine far-field effects have been completed and utilize several models. Beels [11] modeled an array of the Wave Dragon device using MILDwave. The MIKE21 Boussinesq model was calibrated against WEC-Array experimental data by both Nørgaard & Andersen [12] and Angelelli & Zanuttigh [13]. On the spectral side, Silverthorne [5] modified the TOMAWAC source code and added a frequency and directional dependence for transmissivity to model representative WEC performance (RCW) curves. Smith [10] built upon the previous work at the WaveHub site and modified the SWAN source code to include frequency and directional dependent WEC power source terms. However, none of the spectral model studies above were able to be validated against observational data. Alexandre [14] and Porter [9] both compared results of the SWAN model to observed data, however the frequency dependent modifications to the incident wave spectra were completed externally to the program. With the intent of optimizing array design, Child [15] modeled WEC arrays using Garrad Hassan's code WaveFarmer, which was developed from the baseline spectral solver TOMAWAC. Since TOMAWAC and WaveFarmer are commercial codes, their source code modifications are not publicly available, and information on code validation is limited. The authors herein seek to further the previous WEC array work by developing the open source code, SNL-SWAN. The code's development includes creating a WEC-Module in SWAN, and validating its functionality by comparison to an observational data set from the 1:33 scale Columbia Power Technologies Manta 3.1 data collected at Oregon State University's Hinsdale Tsunami Wave Basin (TWB). Earlier work by these authors and others is presented in Ruehl et

al. [16] which verify the functionality of the SWAN source code modifications. The following sections will describe the observational data set collected at the TWB and how it is used to validate SNL-SWAN. This paper will also address whether a spectral model that discretizes the transmission coefficients by frequency bin is better than applying transmission coefficients equally across the frequency spectrum.

## OBSERVATIONAL DATASET

As mentioned above, SNL-SWAN will be validated by the array tests performed by ColPwr at OSU's TWB. In these experiments, WEC array (1, 3, and 5 WECs) performance in monochromatic and simulated real sea states was measured, and wave characteristics were recorded by 23 wave gages (grouped in cross-shore and longshore arrays) located on the seaward and leeward sides of the array. Figure 1 shows the experimental setup with wave gages (circles), WECs (triangles), and Acoustic Doppler Velocimeters (ADVs) (diamonds). Detailed information on the experiments is available in Haller [7] and Porter [9]. This paper focuses on the real seas simulation portions of the experiments, as this is closest to what will be experienced in the field. At field scale the sea states range between peak periods of 7.0 seconds to 12.75 seconds, with unidirectional and directional spreading parameters.

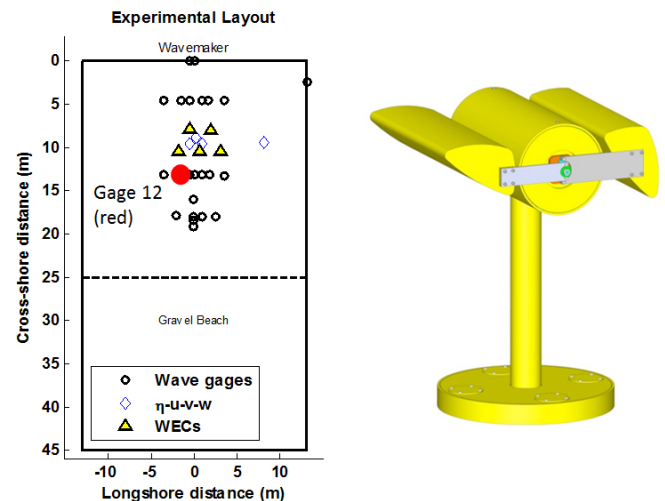


**FIGURE 1 - (A) THE EXPERIMENTAL LAYOUT WITH WAVE GAGES (CIRCLES) AND WECs (TRIANGLES), ADCPS (DIAMONDS). ORANGE WECs INDICATE THE SETUP FOR THE 5-WEC ARRANGEMENT. RED DOT INDICATES LOCATION OF GAGE 12. (B) A RENDERING OF THE COLPWR WEC MANTA 3.1.**

In addition to observed wave data, these experiments provide the WEC performance data

used in this analysis. In this paper the performance data will be defined by the device's Relative Capture Width, which is the relative amount of power extracted from the wave field to the amount available in the width of the device, and is shown in (1).

$$RCW = \frac{P_{absorbed}}{P_{incident,flux}CW} \quad (1)$$

Where  $P_{absorbed}$  is the amount of power absorbed at each frequency,  $P_{incident,flux}$  is the power flux of the incident wave field at each frequency and  $CW$  is a characteristic width (typically equal to device width). Figure 2 shows the qualitative device RCW curve as a function of wave frequency. As was shown in Porter [9], which uses the same TWB data set, the magnitude of the wave reduction behind the array (wave shadow), dependent on the incident sea state, is largely a function of frequency-dependent device performance. Therefore, the device performance curve provides a starting point for modeling the effect that WEC arrays have on the wave climate.

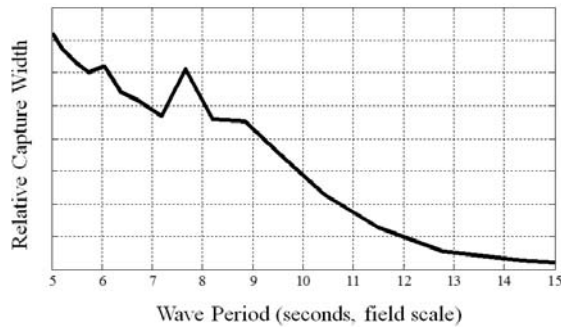


FIGURE 2 - CONCEPTUAL RELATIVE CAPTURE WIDTH PLOT AT LAB SCALE (NOTE: NOT ACTUAL "MANTA" RCW CURVE).

### SNL-SWAN DEVELOPMENT

The Alpha version of the SNL-SWAN WEC Module allows the user to parameterize WEC performance by one of three methods: a constant transmission coefficient, a frequency and wave height dependent transmission coefficient based on a WEC Power Matrix, or a frequency dependent transmission coefficient based on an RCW curve. The constant transmission coefficient can either be chosen by the user, or can be determined by SNL-SWAN. The Alpha version of the WEC Module extracts a transmission coefficient that is associated with the WEC's power performance at the peak period of the incident wave spectra.

Having multiple input options for SNL-SWAN based on typical methods of assessing WEC power performance gives the module more versatility.

Verification of the model with an extensive observed data set gives confidence to the numerically observed environmental effects that may occur due to utility scale wave farms. Because utility scale wave farms are yet to be built, the only method for estimating effects is numerically. Additionally, even when utility scale wave farms are operational, every site is different and will require its own assessment.

Development of SNL-SWAN has occurred in stages because of the complexity of the problem. This section will describe two versions of SNL-SWAN, which build upon baseline SWAN (referred to as SNL-SWAN Alpha and Beta). First, we will describe how SNL-SWAN built upon the traditional obstacle in SWAN. In SNL-SWAN Alpha an equivalent transmission coefficient is calculated and dependent on a user input text file of the WEC's power performance at the peak period of the incident wave spectrum. In this version of the code, there are three WEC Module options:

- 0 = Baseline SWAN (constant transmission coefficient, Kt)
- 1 = WEC Power Matrix
- 2 = WEC Relative Capture Width (RCW) Curve

The user inputs the desired option (0, 1 or 2) in a text file (Width.txt), as well as the device width. This file tells SNL-SWAN Alpha to determine the transmission coefficient based on the defined WEC Module option. Option 0 is a user-defined transmission coefficient in the SWAN input file. Option 1 is the user-specified power matrix file (Power.txt) and the peak period of the incident wave climate. And Option 2 is the user-specified relative capture width (Relative Capture Width.txt) and the peak period of the incident wave climate. Examples of a WEC power matrix and RCW curve are shown in Table 1, and Figure 2, respectively. In this case the y-axis labels are removed from the RCW curve as the performance data is proprietary to ColPwr. The power matrix should be defined in terms of significant wave height ( $H_s$ ) and peak wave period ( $T_p$ ).

TABLE 1 - SAMPLE WEC POWER MATRIX

Mean Power Flux		$T_p$ [s]															
[kW/m]		0.522	0.693	0.870	1.045	1.218	1.392	1.567	1.742	1.916	2.089	2.263	2.437	2.612	2.787	2.961	
$H_s$ [m]	0.0152	0.0000	0.0000	0.0000	0.0000	0.0000	0.0000	0.0000	0.0000	0.0000	0.0000	0.0000	0.0000	0.0000	0.0000	0.0000	
	0.0303	0.0000	0.0000	0.0000	0.0000	0.0000	0.0000	0.0000	0.0000	0.0000	0.0000	0.0000	0.0000	0.0000	0.0000	0.0000	
	0.0455	0.0000	0.0000	0.0000	0.0000	0.0000	0.0000	0.0000	0.0000	0.0000	0.0000	0.0000	0.0000	0.0000	0.0000	0.0000	
	0.0606	0.0000	0.0000	0.0000	0.0000	0.0000	0.0000	0.0000	0.0000	0.0000	0.0000	0.0000	0.0000	0.0000	0.0000	0.0000	
	0.0758	0.0000	0.0000	0.0000	0.0000	0.0000	0.0000	0.0000	0.0000	0.0000	0.0000	0.0000	0.0000	0.0000	0.0000	0.0000	
	0.0909	0.0000	0.0000	0.0000	0.0000	0.0000	0.0000	0.0000	0.0000	0.0000	0.0000	0.0000	0.0000	0.0000	0.0000	0.0000	
	0.1061	0.0000	0.0000	0.0000	0.0000	0.0000	0.0000	0.0000	0.0000	0.0000	0.0000	0.0000	0.0000	0.0000	0.0000	0.0000	
	0.1212	0.0000	0.0000	0.0000	0.0000	0.0000	0.0000	0.0000	0.0000	0.0000	0.0000	0.0000	0.0000	0.0000	0.0000	0.0000	
	0.1364	0.0000	0.0000	0.0000	0.0000	0.0000	0.0000	0.0000	0.0000	0.0000	0.0000	0.0000	0.0000	0.0000	0.0000	0.0000	
	0.1515	0.0000	0.0000	0.0000	0.0000	0.0000	0.0000	0.0000	0.0000	0.0000	0.0000	0.0000	0.0000	0.0000	0.0000	0.0000	
	0.1667	0.0000	0.0000	0.0000	0.0000	0.0000	0.0000	0.0000	0.0000	0.0000	0.0000	0.0000	0.0000	0.0000	0.0000	0.0000	
	0.1818	0.0000	0.0000	0.0000	0.0000	0.0000	0.0000	0.0000	0.0000	0.0000	0.0000	0.0000	0.0000	0.0000	0.0000	0.0000	
	0.1970	0.0000	0.0000	0.0000	0.0000	0.0000	0.0000	0.0000	0.0000	0.0000	0.0000	0.0000	0.0000	0.0000	0.0000	0.0000	
	0.2121	0.0000	0.0000	0.0000	0.0000	0.0000	0.0000	0.0000	0.0000	0.0000	0.0000	0.0000	0.0000	0.0000	0.0000	0.0000	
	0.2273	0.0000	0.0000	0.0000	0.0000	0.0000	0.0000	0.0000	0.0000	0.0000	0.0000	0.0000	0.0000	0.0000	0.0000	0.0000	

The discretized action balance equation (2) in curvilinear coordinates solves for the action

density (N), defined as the energy density per a particular frequency, which is conserved. In the presence of obstacles, the action balance equation includes the time derivative ( $1/\Delta t$ ), diffusion coefficients (D), and source terms such as depth induced breaking (S). The most relevant parameter is the ratio of the incident to lee wave heights, the obstacle transmission coefficient ( $K_t$ ) shown in (3). Baseline SWAN's obstacle transmission coefficient ( $K_t$ ) is squared in the spectral action balance equation, due to the fact that this coefficient represents the ratio of lee to incident wave heights at the obstacle. SNL-SWAN Alpha version parameterizes Options 1 and 2 similarly within the executable. In both cases the WEC Module calculates the incident wave power available to the WEC based on the incident power flux and the device width. Then the ratio of the absorbed power to the incident power is determined based on the WEC's power performance (defined by a power matrix or RCW curve), as shown in (1). The power ratio is then returned to SNL-SWAN as the power transmission coefficient ( $K_{tp}$ ) for the obstacle, as defined in (5), and printed to the swan output file. However,  $K_{tp}$  represents a power ratio, and is therefore not squared in the spectral action balance equation for both of the SNL-SWAN Alpha Options 1 & 2.

$$\begin{aligned} & \left( \frac{1}{\Delta t} + (D_{x,1} + D_{x,2})c_{x,i,j}^+ \right. \\ & \quad + (D_{y,1} + D_{y,2})c_{y,i,j}^+ \left. \right) N_{i,j}^+ \\ & - \frac{N_{i,j}^-}{\Delta t} - D_{x,1}(c_x K_{t,1}^2 N)_{i-1,j}^+ \quad (2) \\ & - D_{y,1}(c_y K_{t,1}^2 N)_{i-1,j}^+ \\ & - D_{x,2}(c_x K_{t,2}^2 N)_{i,j-1}^+ \\ & - D_{y,2}(c_y K_{t,2}^2 N)_{i,j-1}^+ = S_{i,j}^+ \end{aligned}$$

$$K_t = \frac{H_{lee}}{H_{incident}} \quad (3)$$

$$K_{tp} = K_t^2 \quad (4)$$

$$K_{tp} = 1 - RCW \quad (5)$$

SNL-SWAN Beta builds on the Alpha version by allowing the transmission coefficient at each computational grid frequency bin to be determined by the  $K_{tp}$  value calculated at that frequency bin based on the RCW curve. Later versions shall be able to implement the WEC power matrix. Instead of assigning an equivalent transmission coefficient across the frequency spectrum, the WEC Module in SNL-SWAN Beta assigns a transmission coefficient based on the

user-defined WEC power performance to each frequency bin. Inclusion of this calculation procedure is triggered on by additional WEC module options in the width file, in addition to options 0, 1, and 2 above:

3 = RCW Curve with Frequency Variable  $K_{tp}$

4 = Power Matrix with Frequency Variable  $K_{tp}$ <sup>1</sup>

SNL-SWAN Beta also builds on Alpha by providing an output of WEC power (in watts) for each device. Power is estimated by the application of power performance data to the incident wave field for each device.

To date, all of the modifications to the SWAN source code were made to SWAN4072abcde due to its compatibility with DELFT3D, which is commonly used for assessing water quality and sediment transport, especially for artificial environments like harbors and locks. While this is an older version of SWAN, it was determined that more recent releases of SWAN do not have additional features that would significantly impact wave farm modeling. It is likely that as SNL-SWAN is developed further modifications will be integrated into the latest version of SWAN.

#### MODEL-TO-MODEL COMPARISONS

It is important to understand the importance of frequency dependence when selecting transmission coefficients for SWAN obstacles. This section will highlight differences between different versions of the code, and describe the results of these differences. Figure 3 shows normalized<sup>2</sup> wave spectra from two sea states and normalized<sup>3</sup> relative capture width. In baseline SWAN, a transmission coefficient is guessed or chosen based on expected device performance. Using SNL-SWAN Alpha Option 2, the equivalent transmission coefficient is determined based on the RCW value at the peak period of the incident wave period and applied across all wave frequencies. In Figure 3 the RCW values used to determine  $K_{tp}$  for sea states OR2 and OR3 are shown where the vertical black (OR2) and vertical red (OR3) lines intersect with the RCW curve. Clearly the transmission coefficients will be different for the two sea states. Also worth noticing is that the RCW values do not necessarily represent the performance of the device at other

<sup>1</sup> Once Implemented

<sup>2</sup> Wave spectra is normalized by the maximum energy spectra value. The relative shape of the spectra is constant and is not intended to make the curve look like a "normal" curve.

<sup>3</sup> RCW is normalized by the maximum value on the curve

frequencies in the wave spectra. In both of these cases, if the RCW value is chosen based on the peak period only, an over-estimate of the power removed at higher periods, and under-estimate at lower periods will occur. We should then expect to see a larger (perhaps overestimated) shadow with SNL-SWAN Alpha than Beta. This should also be true when comparing the spectral shapes; when the spectra is reduced at an equal proportion across all frequencies in SNL-SWAN Alpha, the reduction at higher periods should be exaggerated, as shown in Figure 3. For this case, baseline SWAN was run with a lower  $K_t$  value than the SNL-SWAN Alpha version had calculated based on the RCW curve value at the peak spectral period. The SNL-SWAN Beta version and OSU Module have frequency dependent energy extraction based on the RCW curve.

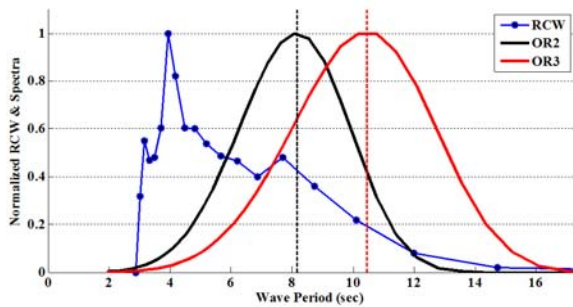


**FIGURE 3 - CONCEPTUAL NORMALIZED RCW CURVE (BLUE CIRCLES), INCIDENT SPECTRA, AND RCW TAKE-OFFS FOR THE OREGON 2 (LEFT, BLACK) AND OREGON 3 (RIGHT, RED).**

An analysis of model results with different model versions and identical incident wave climates should reflect the predictions discussed above. The analysis was completed for sea states and WEC performance coefficients shown in Table 2. In these trials SWAN is run with GEN1 physics, breaking on, bottom friction on default, triads on, quads off, and BSBT propagation on. Incident spectra are defined by peak period and significant wave height in the Pierson-Moskowitz distribution.

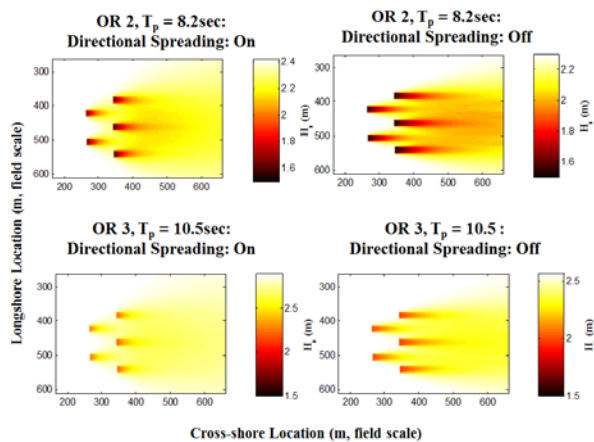
The following comparison is between four approaches to WEC parameterization in SWAN; inputs are summarized in Table 2. The Baseline SWAN cases use a single transmission coefficient that is equal for both sea states. The value of the baseline coefficient cannot be released as it is being compared to proprietary data; however it serves as a reference point for the other model simulations (Alpha, Beta, OSU Module). As with the baseline model the effective transmission coefficient  $K_t$  for SNL-SWAN Alpha cannot be released because it is referenced to a wave period and associated power capture coefficient. In both SNL-SWAN Beta and the OSU-Module the  $K_t$  value will vary by frequency. The OSU-Module is included to serve as an additional reference only, and is expected to perform similarly to SNL-SWAN Beta.

**TABLE 2 - SEA STATE CONDITIONS AND EFFECTIVE TRANSMISSION COEFFICIENTS (KTP) USED FOR THE MODEL-TO-MODEL COMPARISON.**

SWAN version	Sea State	Field Scale $H_s, Target$	Field Scale $T_p, Target$	Directional Spreading <sup>4</sup>	$K_t$
Baseline SWAN	OR2	2.5m	8.2	4, UD	Constant
SNL-SWAN Alpha	OR2	2.5m	8.2	4, UD	Constant based on power performance
SNL-SWAN Beta	OR2	2.5m	8.2	4, UD	Frequency dependent based on power performance
OSU-Module	OR2	2.5m	8.2	4, UD	Frequency dependent based on power performance
Baseline SWAN	OR3	2.5m	10.5	4, UD	Constant
SNL-SWAN Alpha	OR3	2.5m	10.5	4, UD	Constant based on power performance
SNL-SWAN Beta	OR3	2.5m	10.5	4, UD	Frequency dependent based on power performance
OSU-Module	OR3	2.5m	10.5	4, UD	Frequency dependent based on power performance

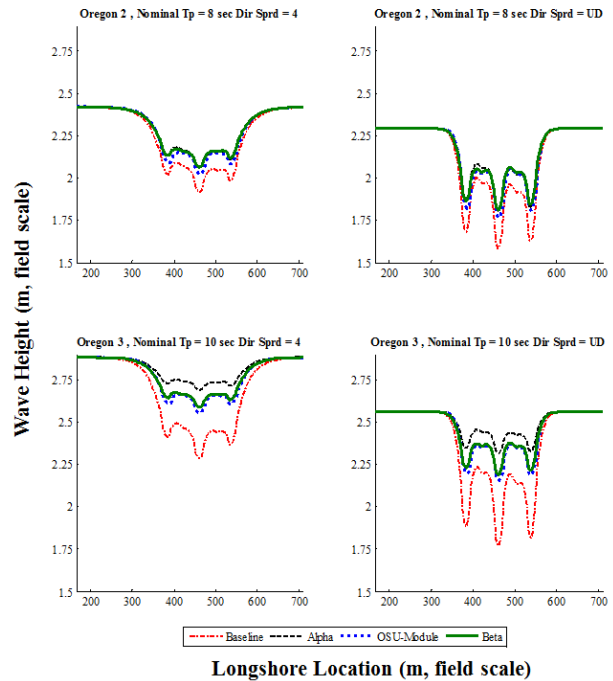
<sup>4</sup> Directional Spreading is parameterized by the  $\cos^{2s}(\theta - \theta_{Peak})$  distribution. In this analysis unidirectional (UD) seas are parameterized by a spreading value of  $s = 40$  in SWAN.

Figure 4 shows a sample of results from the SNL-SWAN Alpha simulations at field scale for directionally spread seas and a parameterization<sup>3</sup> of unidirectional seas. In these figures the incident wave height is varied because the measured incident wave height and the target wave height differed in the observed trials. Therefore the average incident wave height was forced at the boundary with the PM spectrum. Details for determining the incident wave conditions can be found in Porter [9]. The dashed black lines in this figure indicate the location of transects plotted in Figure 5. The shadow magnitude in the Oregon 2 sea state is greater due to the higher RCW value of this device at shorter wave periods, as shown in Figure 3.



**FIGURE 4- SNL-SWAN ALPHA RESULTS FOR THE OREGON 2 AND OREGON 3 SEA STATES WITH VARIABLE SPREADING PARAMETERS. DARKER COLORS INDICATE MORE SHADOWING.**

Wave height transects showing results from Baseline SWAN, SNL-SWAN Alpha, SNL-SWAN Beta, and the OSU-Module are shown in Figure 5. As discussed earlier, shadowing in SNL-SWAN Alpha (black dashed line) is over-predicted as compared to SNL-SWAN Beta and OSU (blue dashed line) when using the same device input. The reference line from Baseline SWAN (red) results in more shadowing than any of the models because a lower  $K_t$  value was chosen. Diffraction in these simulations has not been enabled, therefore the shadow transects appear exaggerated. To isolate differences in model device representation differences we can look at the shape of the energy spectra.



**FIGURE 5 - WAVE HEIGHT TRANSECTS OF THE DIFFERENT MODEL VERSIONS FOR TWO INCIDENT WAVE STATES (OR2 AND OR3) AT TWO DIFFERENT DIRECTIONAL SPREADING PARAMETERS (S = 4, AND UNIDIRECTIONAL).**

The essential difference between WEC parameterization between constant transmission and frequency dependent transmission is shown in the conceptual comparison in Figure 6, where the spectral shape is preserved in SWAN and SNL-SWAN Alpha, but not in SNL-SWAN Beta. The differences are most pronounced directly in the lee of the device, where the peak of the spectra in SNL-SWAN Beta is flattened. This will be evidenced not just at the WEC, but in the lee of the array as well.

As distance in the lee of the array increases, the effect becomes more muted due to lateral energy spreading. However, Figure 7 shows that in the lee of the array differences in spectral shape are visible between models. SNL-SWAN Alpha and Baseline SWAN both maintain shape, but SNL-SWAN Beta and the OSU-Module undergo shifts. These spectra were recorded in the model at the location of wave gage 12 [9] shown in the left panel of Figure 1. This location was chosen because it is nearly directly in the lee of a WEC, and can be compared to measured spectra in the observational data set. The spectra shape change signal measured here is not expected to be as strong in directly at the WEC, which is shown in

Figure 6; significant shadow attenuation is seen in Figure 4 in the lee of the WECs.

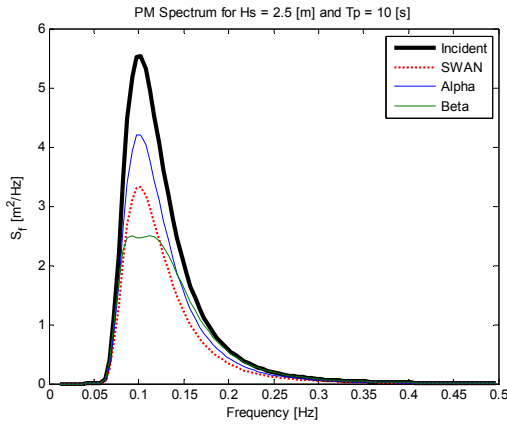


**FIGURE 6 - CONCEPTUAL COMPARISON OF SPECTRAL TRANSFORMATION USING BASELINE SWAN (RED), SNL-SWAN ALPHA (BLUE) AND SNL-SWAN (BETA) GREEN DIRECTLY AT LEE OF WEC.**

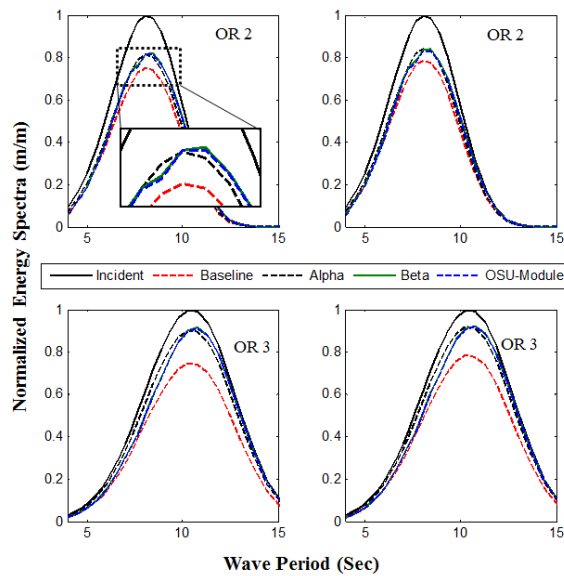


**FIGURE 7 - ENERGY SPECTRA AT GAGE IN THE LEE OF THE WEC-ARRAY FOR OR 2 (TOP) AND OR3 (BOTTOM) AND DIRECTIONAL SPREADING ON (LHS) AND OFF (RHS).**

**PRELIMINARY SNL-SWAN MODEL VALIDATION**

Results from the previous section are compared to the observational data set. The preliminary validation with the observational data set is limited, with two of the seven possible sea states investigated, and only 5-WEC arrangement. However the 5-WEC arrangement gives the largest signal-to-noise ratio so is best for comparison to observations. Figure 8 shows wave height cross section with the addition of observed data with

green circles. It is clear that the frequency bin dependent models give overall a better estimate of shadowing. As was shown before in [9], at shorter wave periods, which are more present in OR2 than OR3, the shadowing becomes a function of wave scattering as well as absorption. Therefore the shadowing is underestimated more in sea states with a shorter peak period.

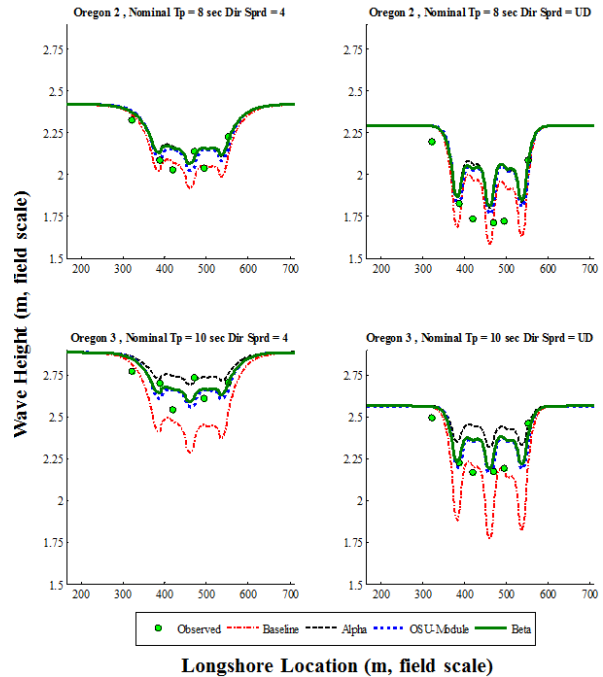


**FIGURE 8 - WAVE HEIGHT TRANSECTS OF OBSERVATIONS AND MODEL ITERATIONS FOR TWO INCIDENT WAVE STATES (OR2 AND OR3) AT TWO DIFFERENT DIRECTIONAL SPREADING PARAMETERS (S = 4, AND UNIDIRECTIONAL).**

The comparison of observed spectral shape changes to model results at wave gage 12 is shown in Figure 9. The spectra are presented at an interval of  $0.05s^{-1}$  and 48 degrees of freedom. Given that, it is still clear that the observed wave climate in the lee is frequency dependent by how the observed data reduction fluctuates with respect to the incident spectra. It is also clear that the measured energy spectra in the lee of the array are complex. We see that at shorter wave periods the shadowing is not entirely captured by the gaps between measured and simulated.

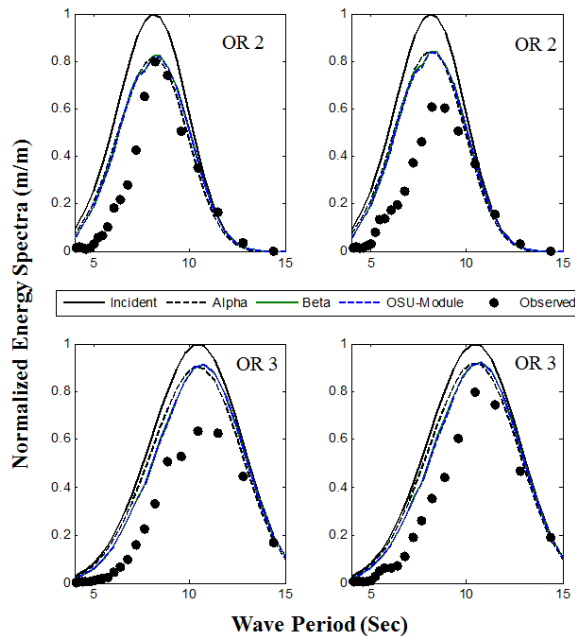


**FIGURE 9 - ENERGY SPECTRA AT GAGE IN THE LEE OF THE WEC-ARRAY FOR OR 2 (TOP PANELS) AND OR3 (BOTTOM PANELS) AND DIRECTIONAL SPREADING ON (LEFT PANELS) AND OFF (RIGHT PANELS).**

### CONCLUSIONS AND FUTURE WORK

Preliminary comparisons, using limited observational data, have shown that the SNL-SWAN Alpha and Beta models simulate the lateral wave height diffusion in the lee of WEC arrays in wave fields with directionally spread seas reasonably well. In this analysis, typically the wave shadow magnitude was less in SNL-SWAN Alpha and greater in the OSU-Module and SNL-SWAN Beta. This is due to the nature of the RCW curve for this device and the peak wave periods of the incident wave climates. For other wave climates, the trend could be the opposite. Limited investigation showed that frequency bin dependent models such as the OSU-Module and SNL-SWAN Beta predict the wave height shadow in the lee of the array better when compared to observational data wave height transects, but still underestimate the total magnitude. Limited analysis of changes to the spectral shape in the lee of the device relative to incident showed that differences were apparent between models. The comparison of this analysis to observed spectra is limited, but it demonstrates the complexity of the observed lee spectra shape. Additionally, the shadowing effect at short (<8 seconds at field scale) wave periods is underestimated by the Alpha version of SNL-SWAN.

To close the gap between observed spectral shape and wave shadow for a wide range of sea states SNL-SWAN will continue to be developed, perhaps including a frequency dependent reflection coefficient, or other parameterization of scattered waves. Testing of SNL-SWAN Beta will build on the present limited comparison with a more broad comparison to the TWB data set. Limited SNL-SWAN Beta releases will provide additional testing of the model that will be used to further the development of open-source SNL-SWAN code to include modifications based on input from the users.

### ACKNOWLEDGMENTS

This research was made possible by support from the Department of Energy's EERE Office's Wind and Water Power Technologies Office. The work was supported by Sandia National Laboratories, a multi-program laboratory managed and operated by Sandia Corporation, a wholly owned subsidiary of Lockheed Martin Corporation, for the U.S. Department of Energy's National Nuclear Security Administration under contract DE-AC04-94AL85000. Special thanks to Craig Jones, Grace Chang, and Jason Magalen at Sea Engineering Inc. for their support on development of SNL-SWAN, to Merrick Haller at Oregon State University for his support on the OSU testing, and to Ken Rhinefrank and Pukha Lenee-Bluhm at Columbia Power Technologies for their characterization data of the Manta 3.1 WEC.

### REFERENCES

- [1] "TU Delft: The official SWAN Home Page - [www.swan.tudelft.nl](http://www.swan.tudelft.nl)." [Online]. Available: <http://www.swan.tudelft.nl/>.
- [2] Agamloh, E.B., Wallace, A.K., von Jouanne, A., 2008. Application of fluid-structure interaction simulation of an ocean wave energy extraction device. *Renew. Energy* 33, 748-757.
- [3] C. McNatt, "Wave Field Patterns Generated by Wave Energy Converters," Oregon State University, Corvallis, Oregon, 2012.
- [4] M. Folley, A. Babarit, B. Child, D. Forehand, L. O'Boyle, K. Silverthorne, J. Spinneken, V. Stratigaki, and P. Troch, "A Review of Numerical Modelling of Wave Energy Converter Arrays," in *Proceedings of the ASME 2012 31st International Conference on Ocean, Offshore and Arctic Engineering*, Rio de Janeiro, Brazil, 2012.
- [5] K. E. Silverthorne and M. Folley, "A New Numerical Representation of Wave Energy Converters in a Spectral Wave Model," in *EWTEC 2011*, Southampton, UK, 2011.

- [6] Millar, D., Smith, H. & Reeve, D. (2007) Modelling analysis of the sensitivity of shoreline change to a wave farm. *Ocean Engineering* 34(5-6):884-901.
- [7] M. Haller, A. Porter, P. Lenee-Bluhm, K. Rhinefrank, E. Hammagren, T. Ozkan-Haller, and D. Newborn, "Laboratory Observations of Waves in the Vicinity of WEC-Arrays," in EWTEC 2011, Southampton, UK, 2011
- [8] Venugopal, V. & G.H. Smith, "Wave climate investigation for an array of wave power devices", in Proceedings of 7th European Wave and Tidal Energy Conference, Porto, Portugal, 2009
- [9] A. Porter, "Laboratory Observations and Numerical Modeling of the Effects of an Array of Wave Energy Converters," Oregon State University, Corvallis, Oregon, 2012.
- [10] H. C. M. Smith, C. Pearce, and D. L. Millar, "Further analysis of change in nearshore wave climate due to an offshore wave farm: An enhanced case study for the Wave Hub site," *Renew. Energy*, vol. 40, no. 1, pp. 51–64, Apr. 2012.
- [11] C. Beels, P. Troch, K. De Visch, J. P. Kofoed, and G. De Backer, "Application of the time-dependent mild-slope equations for the simulation of wake effects in the lee of a farm of Wave Dragon wave energy converters," *Renew. Energy*, vol. 35, no. 8, pp. 1644–1661, Aug. 2010.
- [12] J. H. Nørgaard and T. L. Andersen, "Investigation of wave transmission from a floating wave dragon wave energy converter," presented at the Proceedings of the 22nd International Offshore and Polar Engineering Conference. Rhodes, 2012.
- [13] E. Angelelli, B. Zanuttigh, and J. P. Kofoed, "Numerical modelling of the hydrodynamics around the farm of Wave Activated Bodies (WAB)," in ICOE 2012, Dublin, Ireland, 2012.
- [14] A. Alexandre, T. Stallard, and P.K. Stansby, "Transformation of Wave Spectra across a Line of Wave Devices," in Proceedings of the 8th European Wave and Tidal Energy Conference, Uppsala, Sweden, 2009
- [15] Child, B. F. M. and Weywada, "Verification and validation of a wave farm planning tool", in EWTEC 2013, Aalborg University, Denmark
- [16] K. Ruehl, A. Porter, A. Posner, J. Roberts, "Development of SNL-SWAN, a Validated Wave Energy Converter Array Modeling Tool" in EWTEC 2013, Aalborg University, Denmark